Food and Chemical Toxicology 136 (2020) 111081

Contents lists available at ScienceDirect

Food and Chemical Toxicology

journal homepage: www.elsevier.com/locate/foodchemtox

Detection of zearalenone in an aptamer assay using attenuated internal reflection ellipsometry and it's cereal sample applications

Mustafa Oguzhan Caglayan[a,*], Zafer Üstündağ[b]

[a] Bilecik Seyh Edebali University, Bioengineering Department, Bilecik, Turkey
[b] Kutahya Dumlupinar University, Chemistry Department, Kutahya, Turkey

ARTICLE INFO

Keywords:
Zearalenone (ZEN)
Cereal samples
Aptamer
Attenuated internal reflection spectroscopic ellipsometry (AIR-SE)
Surface plasmon resonance (SPR)

ABSTRACT

Mycotoxins are toxic compounds produced by the metabolism of certain fungi that threaten the food and agricultural industry. Over hundreds of mycotoxins, one of the most common toxins, zearalenone (ZEN), has toxic effects on human and animal health due to its mutagenicity, treatogenicity, carcinogenicity, nephrotoxicity, immunotoxicity, and genotoxicity. In this work, attenuated internal reflection spectroscopic ellipsometry (AIR-SE) combined with the signal amplification via surface plasmon resonance conditions that were proved to be a highly sensitive analytical tool in bio-sensing was developed for the sensitive and selective ZEN detection in cereal products such as corn, wheat, rice, and oat. Combined with the oligonucleotide aptamer for ZEN recognition, our proposed method showed good performance with yielding 0.08 ng/mL LOD and 0.01–1000 ng/mL detection range. A mini-review was also introduced in, to compare various methods for ZEN detection.

1. Introduction

Mycotoxins are secondary metabolites of fungi and have been a major concern in the food and agricultural industry. These fungi colonize on crops either during harvesting or during storage and cause financial problems due to food lost, as well as it poses a significant health risk to the consumer of contaminated products (Chauhan et al., 2016). Unfortunately, these toxins are resistant to processing temperatures and have a tendency to remain in the food chain (Kabak, 2009). There are hundreds of fungal toxins have been identified so far, among them, a relatively small number of toxins threaten food safety (Mak et al., 2010). The major fungi genera threaten food safety are *Aspergillus*, *Alternaria*, *Fusarium,* and *Penicillium* (Shephard, 2008), whose toxins should be detected by means of rapid and sensitive methods. The detection of these toxins in foodstuff and animal feeds is a vital concern due to both widespread occurrence and severe life-threatening effects of fungal contamination, including, teratogenic, mutagenic, nephrotoxic, immunosuppressive and carcinogenic behavior (Rodrigues et al., 2011). The maximum residue limits for major toxins have already been established by authorities which are as low as 2 ppm (Alshannaq and Yu, 2017). The residual mycotoxins can be found not only in crops but also in dairy products and alcohols which are produced from contaminated agricultural crops (Goud et al., 2018).

Current analytical methods for the detection and quantification of mycotoxins include thin-layer chromatography, or fluorescence and chemiluminescence techniques, high-performance liquid chromatography, or enzyme-linked immunosorbent assays (ELISAs) (Daly et al., 2000). However, these analytical methods are unsuitable for on-site monitoring even their sensitivity and selectivity are good enough. Moreover, these methods have some drawbacks including the requirement for professional analysts to operate delicate instruments or complex analytical methods. Consequently, hundreds of various methods have been developed for mycotoxin detection according to the requirement for continuous monitoring of residual mycotoxins in food products.

There are valuable review articles have focused on electrochemical sensors (Goud et al., 2018), electrochemical biosensors (Fernández et al., 2017), aptasensors (Sharma et al., 2015), microchip-based sensors (Man et al., 2017), electromigration and lateral flow sensors (Li et al., 2012), SPR immunosensors (Meneely and Elliott, 2014) used for food safety.

Zearalenone (ZEN), metabolites of Fusarium species, is a mycotoxin that threatens food safety which can be found in the majority of grain crops. As other mycotoxins, ZEN is classified as a nonsteroidal estrogen (Bennett and Klich, 2003), with hepatotoxicity, haematotoxicity, immunotoxicity (Vlata et al., 2006), and genotoxicity (Collins et al., 2006). It has also been associated with the hyperplasic and neoplasic endometrium and human cervical cancer (Zinedine et al., 2007).

* Corresponding author.
E-mail addresses: caglayanmoguzhan@gmail.com, oguzhan.caglayan@bilecik.edu.tr (M.O. Caglayan).

https://doi.org/10.1016/j.fct.2019.111081
Received 20 September 2019; Received in revised form 12 December 2019; Accepted 23 December 2019
Available online 26 December 2019

Maximum residual ZEN levels have been set by regulations is as low as 20 ng/g for baby foods (EU Regulation 856/2005 (Hervás et al., 2011);).

Similar to other mycotoxins, the common analytical method for the quantification of ZEN is LC-MS (Liu et al., 2018; Ren et al., 2018; Yan et al., 2018). However, this golden analytical technic requires sophisticated equipment, labor-intensive recipes, and time-consuming steps.

There are various approaches in the relevant literature to detect ZEN residue in food and agricultural products. Immuno-affinity assays and oligonucleotide aptamers have been reported for various transducer and biosensor configurations. These methods are criticized in the Conclusion section of this paper.

In this study, we decided to use an aptamer-based biosensor, since its unique properties among immuno-based approaches. Aptamers are single-stranded oligonucleotides with impressive recognition features (Yang et al., 2011). Aptamers have been developed mainly through the in vitro selection process referred to as the systematic evolution of ligands by exponential enrichment (SELEX) (Sharma et al., 2015; Tuerk, 1997).

Optical biosensors have received considerable attention as non-destructive, simple, and sensitive sensing tools for the detection of toxins (Lee et al., 2018; Wu et al., 2018). In this regard, attenuated internal reflection spectroscopic ellipsometry (AIR-SE) which is intrinsically sensitive to dielectric constant changes on the coupler and dielectric medium interface (Fig. 1), has become prominent. Especially, in combination with surface plasmon resonance (SPR) conditions, this method can reach an as low limit of detection (LOD) as pM for even small molecules (Bombarová et al., 2015).

In this study, we proposed an aptasensor to detect ZEN in food samples in which the AIR-SE method employed under SPR conditions. Also, we criticized recent methods for the detection of ZEN in food samples, at the end of this paper.

2. Experimental

Zearalenone (ZEN, 6-[10-hydroxy-6-oxo-*trans*-1-undecenyl]- β-resorcyclic acid lactone), Tween 20, buffer solution agents, surface modification agents, and other chemicals were purchased from the local representative of Sigma-Aldrich, Riedel and Merck Company. Phosphate buffer saline (PBS) at pH 7.4 (10 mM) contains 0.8% NaCl (w/v) or additionally contains Tween 20 (0.05% v/v) were freshly prepared by using ultra-pure water (HumanPower, 1 +, 18.2 MΩ cm, S. Korea). Aptamer sequence which is 3′ -thiol modified form were purchased from TIB Molbiol (Germany). anti-ZEN aptamer, 3′–SH–T_{10}-TCAT CTAT CTAT GGTA CATT ACTA TCTG TAAT GTGA TATG- 5′ selected from the literature (Chen et al., 2013). Non-complementary aptamer sequence was 3′–SH–T_{10}- CATA CATA GCCG ATCG AAAA TTAA TACA GTAG CATA GCGC-5′.

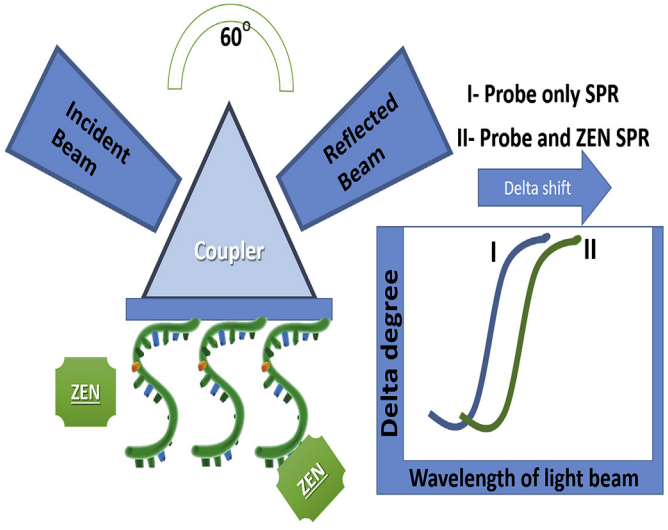

Fig. 1. Schematic diagram of measurement technique of AIR-SE under SPR conditions.

AIR-SE measurements were done using Optosense S2000 model spectroscopic ellipsometer (USA) with flow cell and SPR coupler setup. A Bioforce model UV-ozone cleaner (USA) was used for surface cleaning and modification purposes. All measurements were performed at room temperature which was controlled with conditioning equipment (22 ± 1 °C). At least 3 replicates were done to fulfill analytical requirements.

2.1. Immobilization protocol

3′-SH modified aptamers in PBS buffer were immobilized on Au coated glass slides (BK7 glass) via –SH route. Immobilization duration and probe concentration were optimized using various probe concentrations. Mercaptohexanol was co-immobilized on an aptamer immobilized surface to prevent nonspecific interactions between probe and Au surface.

2.2. AIR-SE setup under SPR conditions

A Kretschmann coupler was used for SPR conditions. AIR-SE conditions were selected to match SPR conditions on 50 nm Au coating. SE-ellipsometer was set at 530 nm wavelength and 60° angle of incidence (Caglayan et al., 2013). A flow cell was set under the incident beam to detect ellipsometric angle delta (Δ) and continuous measurements were done. Samples were injected into the flow-cell by means of a peristaltic pump which was operated at 5 μL/min.

2.3. Precision and accuracy

Precision and accuracy of the developed method were determined by using 5 independent series on the same day for intra-day precision, and 7 consecutive days for inter-day precision from 5 measurements of every series.

2.4. Non-specific interactions

Non-specific interactions were evaluated using ochratoxin A (OTA), ochratoxin B (OTB), aflatoxin B1 (AFB1). Interference tests were done by adding 5000 ng/mL possible interfering agents in ZEN analyte samples (500 ng/mL).

2.5. Real sample analysis

For spiking tests, cereal samples were prepared according to reports elsewhere (Zhan et al., 2016). Briefly, the ZEN solution (in methanol) at determined concentrations was added to 5 g grounded cereal samples to get final ZEN levels. Then samples were extracted using 20 mL methanol: water (80:20) mixture while shaking at room temperature for 30 min. The supernatant was centrifuged and transferred into 10 mM PBS, then injected into the flow-cell. The spiked samples were assayed using the AIR-SE method described above.

3. Results and discussion

3.1. Immobilization of anti-ZEN probes

SH modified anti-ZEN aptamer probe was immobilized on the Au surface, by changing aptamer concentration in buffer and immobilization time. The ellipsometric thickness of the immobilization surface for definite time intervals was determined using ellipsometric measurements by modeling psi (Ψ) and delta (Δ) data. Ellipsometric thickness

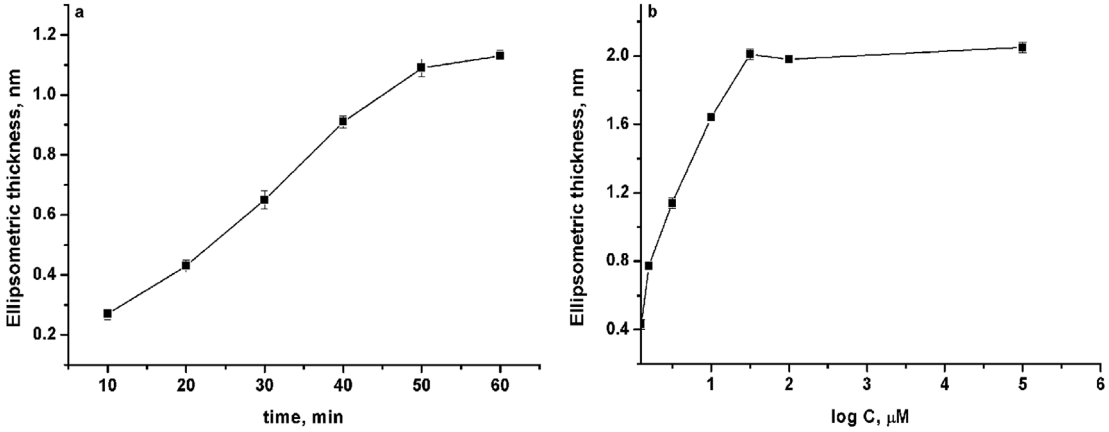

Fig. 2. (a) Ellipsometric thickness evaluation of sensor surface during the immobilization (for 0.5 μM probe), and (b) ellipsometric thickness for various probe concentrations (at 60 min immobilization).

was calculated using equipment built-in software by modeling, according to multilayer model parameters for the Air/Organic layer (n = 1.46)/Au layer/Cr layer/BK7 substrate. Thickness evaluation for the 0.5 μM probe was evaluated at between 10 and 60 min. According to the immobilization duration, the mid-range concentration of anti-ZEN aptamer immobilization has saturated at approximately 50–60 min (Fig. 2a). After that, we decided for 60 min immobilization time is adequate for all immobilization steps in this study.

Another parameter that affected the surface coverage of the probe was the concentration of anti-ZEN, which, in turn, was optimized between 0.1 and 5 μM (Fig. 2b). The optimum concentration at room temperature was 1.2 μM for 60 min.

Furthermore, the blocking agent (MCH) immobilization conditions (concentration and time) were selected according to previous studies (Caglayan, 2018).

3.2. AIR-SE sensor performance

ZEN solutions in buffer were prepared at concentrations ranging from 0.01 ng/mL to 1000 ng/mL. Interaction between the probe and ZEN was monitored at a 60° angle of incidence with 530 nm light. Au surface at SPR conditions has exhibited a sudden change in the Δ parameter. At definite angle and wavelength, Δ has shifted to lower degrees upon binding (or molecular deposition) on the sensor surface. The time-dependent relative Δ change upon ZEN/anti-ZEN interaction is given in Fig. 3a. Relatively high affinity was observed at higher ZEN concentration. Furthermore, Δ values at plateau (after 50 min) were used for the calibration curve of the AIR-SE sensor which is given in Fig. 3b.

According to the calibration curve, the interaction between the anti-ZEN aptamer on the sensor surface and the captured ZEN molecules has taken place in a single site, and the binding rate has decreased with the amount of the free aptamer on the surface. The calibration curve exhibits a wide linear range between 0.01 ng/mL and 1000 ng/mL with a high regression coefficient (Table 1). The calibration curve equation is also reported with standard error values, in Table 1. LOD and limit of quantification (according to 3σ) was 0.08 ng/mL and 0.24 mg/mL, respectively.

The sensor response was highly satisfactory in terms of sensor performance and was comparable to conventional ELISA methods (with a detection limit of 40 pg/mL, reported in Table 4).

3.3. Precision and accuracy

For the precision and accuracy test of the developed method, 0.1, 5.0, and 100 ng/mL of ZEN standard solution was measured in five independent series of an assay for intra-day precision. The relative standard deviation (RSD, as a percentage) and accuracies (as a percentage) are given in Table 2. The RSD was in between 2.26% and 3.39%. The accuracy was also between 0.40% and −2.37%. These results exhibited that the proposed sensor and developed method have high precision and accuracy in terms of intra-day precision. Furthermore, inter-day precision results were in good agreement with the intra-day values and also were in the range between acceptable levels. Both inter-day and intra-day results showed that the proposed method is relatively accurate and precise.

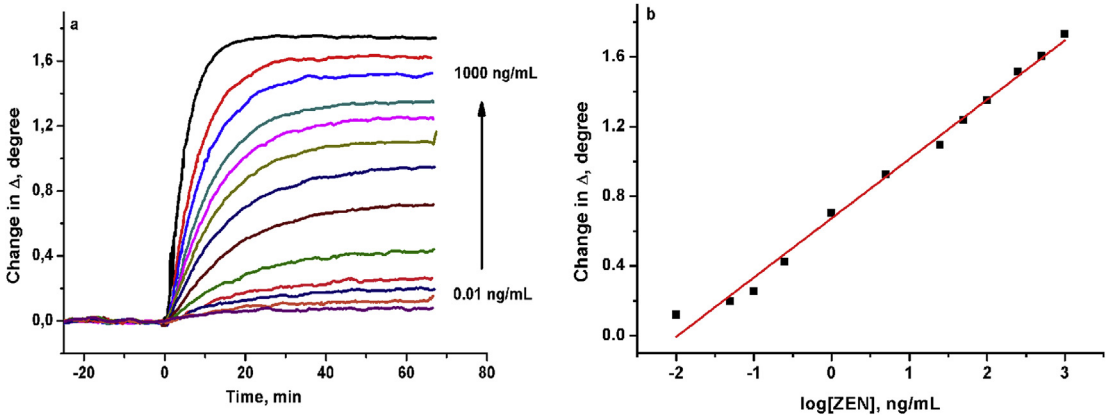

Fig. 3. (a) The time dependent relative Δ change upon ZEN/anti-ZEN interaction (b) and calibration curve.

Table 1
Summary of analytical performance of the proposed method (n = 6).

Analytical characteristic	Values
Linearity range	0.01–1000 ng/mL
Regression equation, Δ (degree) and [ZEN] (ng/mL)	Δ = 0.67351 + 0.34026 [ZEN]
Standard error of the slope, ±	0.01015
Standard error of the intercept, ±	0.01816
R^2	0.9903
LOD, ng/mL	0.08
LOQ, ng/mL	0.24

3.4. Non-specific interactions

The specificity of the proposed AIR-SE aptasensor was determined by possible interferents including OTA, OTB, and AFB1. These toxins are analogs of ZEN mycotoxin. All interferents were added 10-fold excess of proposed analyte ZEN (i.e. 500 ng/mL vs 5000 ng/mL). The signal change percentage of sensor response for specific analyte vs. nonspecific counter molecules was reported as the specificity of the sensor (Table 3). Relative sensor response change upon interferent addition was below 4.8%, which was in acceptable limits for specificity purposes.

3.5. Real sample analysis

Sensor performance on the real sample was evaluated using a known amount of ZEN spiked in cereal samples (Table 4). Spiked amount of ZEN standard was in the mid-range of the calibration curve, which are 1, 5 and 100 ng/mL. The recovery percentages were between 104.7% and 95.2% for cereal individual specimens. These results were in good correlation with the accuracy and precision result which was acquired from ZEN in buffer solution. This result also highlighted that the real sample performance was as high as the synthetic sample performance for the proposed sensor. Also, this recovery result was in the range of acceptable levels.

4. Conclusion

We proposed a highly sensitive and reliable aptasensor for the detection of ZEN in food samples. This AIR-SE sensor under SPR conditions fulfilled our expectations in terms of selectivity, sensitivity, accuracy, and real sample performance. As expected, SPR conditions resulted in a highly acceptable LOD (0.08 ng/mL) and LOQ (0.24 ng/mL) values, which also comparable with the current methods that have been reported in the relevant literature. Furthermore, the quantification range which was between 0.01 and 1000 ng/mL was also competitive with the currently reported methods. Both the accuracy and precision test of the proposed sensor were also quite satisfying and deviations were below 5% for both intra-day and inter-day tests. The specificity of the developed sensor was also high due to the inherent advantages of the aptamer. Non-specific interactions of analog of ZEN molecule (i.e. OTA, OTB, AFB1) were within limits of the repeatability of the sensor. Also, real sensor performance was highly accurate in terms of recovery and was below ± 5% of deviation.

Table 3
The influences of some analogous mycotoxins interferents on the % Δ change of the signal acquired from 500 ng/L ZEN.

Interferents added*	Concentration (ng/mL)	Δ signal change upon interferent addition (%)
OTA	5000	−4.6
OTB	5000	+2.3
AFB1	5000	+4.8

Table 4
Analytical recovery of the proposed sensor in cereal samples (N = 6).

Samples		Spiked amount (ng/mL)	Detected by AIR-SE (ng/mL)	Recovery (%)
Corn-A	I	1.00	1.04	104.0
		5.00	4.87	97.4
		100.0	101.6	101.6
	II	1.00	0.98	98.0
		5.00	4.76	95.2
		100.0	103.8	103.8
Wheat-A	I	10.0	10.05	100.5
		30.0	30.08	100.3
		60.0	58.61	97.7
	II	10.0	10.47	104.7
		30.0	30.43	101.4
		60.0	57.81	96.3
Rice	I			
		5.00	4.87	97.4
		10.0	9.93	99.3
		50.0	48.81	97.6
	II	5.00	5.21	104.2
		10.0	9.68	96.8
		50.0	47.60	95.2
Oat	I	5.00	4.88	97.6
		20.0	20.12	100.6
		100.0	104.17	104.2
	II	5.00	5.07	101.4
		20.0	19.54	97.7
		100.0	96.48	96.5

Some of the relevant literature for ZEN detection in food samples is summarized in Table 5. The novelty of sensor structure and assembly, applied method, calibration range, and LOD are listed in this table. Most of these studies are immunoassays and quite prone to exhibit disadvantages of immune-based recognition elements such as stability, production difficulties and even ethical issues due to animal abuse. Some of the electrochemical methods reported herein (Nasir and Pumera, 2014; Liu et al., 2014), on the contrary, report a direct detection method. The inherent advantages of aptamers such as easiness of their production and purification methods are still relevant due to the selective and sensitive detection capability. Electrochemical sensors that were reported herein, need some nanoparticle aid to achieve a lower limit of detection. However, as expected, achieved lower LOD in turn results in a low detection range. For instance, a 0.001 pg/mL ZEN detection limit has been reported by photoelectrochemical sensor structure, where the detection range was between 10^{-6} and 10 ng/mL (Liu et al., 2017). Other studies on electrochemical based sensors listed in Table 5 have LOD limit between 1.7 pg/mL and 0.58 ng/mL, where

Table 2
Precision and accuracy results of the developed method for ZEN (N = 5).

Added ZEN, ng/mL	Intra-day			Inter-day		
	Found Value, ng/mL	RSD %	Accuracy %	Found Value, μmol/L	RSD %	Accuracy %
0.1	0.098 ± 0.003	3.06	−2.00	0.103 ± 0.002	1.94	+3.00
5.0	5.02 ± 0.17	3.39	+0.40	4.87 ± 0.15	3.08	−2.60
100	97.63 ± 2.21	2.26	−2.37	100.2 ± 2.6	2.59	+0.20

Table 5
Response of various nanosensors for ZEN in literature.

	Method	Novelty/Sensor Structure	Calibration range	LOD	Ref.
1	Electrochemical	GCE-MWCNT- chitosan- BSA-Antibody	0.01–1000 ng/mL	4.7 pg/mL	Xu et al. (2017)
2	Electrochemical	Antibody, alkaline phosphatase linked sandwich, ELISA	0.004–9.5 ng/mL	2 pg/mL	Wang et al. (2013)
3	Electrochemical	BEL-7402 cells, immobilized on GCS, AuNP, p-aminothiophenol and folic acid	0.1–50 μg/mL	IC_{50} 24.6 μg/mL	Gu et al. (2015)
4	Electrochemical	Edge-plain pyrolytic graphite electrode	0.209–17.96 μM	NR	Nasir and Pumera (2014)
5	Electrochemical	M270 Magnetic nanoparticles, biotin/streptavidin-HRP, ELISA	0.07–2.41 ng/mL	40 pg/mL	Zhang et al. (2015)
6	Electrochemical	Magnetic polymer beads, SPE, HRP, immunosensor	0.01–10000 ng/mL	7 pg/mL	Hervas et al. (2010)
7	Electrochemical	Magnetic polymer beads, Protein G, BSA, immunosensor, GCE	0.01–10000 ng/mL	11 pg/mL	Hervas et al. (2009)
8	Electrochemical	AuNP immobilized on MWCNT/polyethyleneimine dispersions. CSPE	10^{-4}-0.1 ng/mL	0.15 pg/mL	Riberi et al. (2018)
9	Electrochemical	Mesoporous carbon and Au@AgPt core-shell NPs	0.005–15 ng/mL	1.7 pg/mL	Liu et al. (2014)
10	Electrochemical	Magnetic bead, immunosensor, GC, microfluidic	0.01–1000 ng/mL	0.4 ng/mL	Hervás et al. (2011)
11	Electrochemical	Magnetic bead, immunosensor, microfluidic	NR	1 ng/mL	Hervás et al. (2009)
12	Electrochemical	Magnetic bead,	NR	0.41 ng/mL	Panini et al. (2011)
13	Electrochemical	Hep G2 cells immobilized on SPCE, AuNP, cystamine, laminin system	0.1–50 μg/mL	IC_{50} 59 μg/mL	Xia et al. (2017)
14	Electrochemical	CPE, MWCNT	2.0–50.0 ng/mL	0.58 ng/mL	Afzali et al. (2015)
15	Electrochemical	Poly-dopamine TiO_2 and Co_3O_4 mezocrystals, photoelectrochemical	10^{-6}-20 ng/mL	0.001 pg/mL	Liu et al. (2017)
16	Fluorescence	Anti-ZEN aptamer, magnetic NPs	0.05–100 ng/mL	7 pg/mL	Wu et al. (2017)
17	Fluorescence	Fluorescence polarization immunoassay	150–1000 ng/g	137 ng/g	Chun et al. (2009)
18	Fluorescence	Modified cyclodextrins, capillary electrophoresis	5–500 ng/g	5 ng/g	Maragos and Appell (2007)
19	Fluorescence	Automated microchannel sensor, ELISA	0.019–0.422 ng/mL	7 pg/mL	Urraca et al. (2005)
20	Fluorescence	Immunosensor, microfluidic, multi-analysis	0.08–7.47 ng/mL	0.01 ng/mL	Wang et al. (2012)
21	Fluorescence	Magnetic bead, flow cytometry, inhibition immunoassay	~0.1–100 ng/mL (NR/from calibration graph)	5.8 ng/mL	Peters et al. (2013)
22	Fluorescence	C18 silica gel bead, solid phase concentration to signal amplification	50–600 ng/mL	15 ng/mL	Llorent-Martínez et al. (2019)
23	Fluorescence	HEK293 cells, TRE-GFP and ERE-RFP plasmids introduced in	10–100 ng/mL	3.2 ng/mL	Ji et al. (2016)
24	Colorimetric	Anti-ZEN aptamer, AuNPs	10–250 ng/mL	10 ng/mL	Sun et al. (2018)
25	Colorimetric	Colloidal Au, Lateral flow immunoassay	1–50 ng/mL	1 ng/mL	Liu et al. (2012)
26	Colorimetric	Immunochromatographic assay, AuNP, nitrocellulose membrane	0.4–20 ng/mL (NR/from spike data)	1 ng/mL	Li et al. (2013)
27	Interferometry	Epoxy coated glass slides, BSA, competitive inhibition, immunoassay	~0.2–100 ng/mL (NR/from calibration graph)	0.48 ng/mL	Orlov et al. (2017)
28	Magnetoresistivity	Magnetic nanotagged immunoassay	0.05–50 ng/mL	50 pg/mL	Mak et al. (2010)
29	HPLC-MS/MS	Extraction method	2–100 ng/mL	40 pg/mL	Chen et al. (2017)
30	SERS	AuNP + Raman Reporter, Immunoassay	10 pg/mL-10 ng/mL	53 ng/g	Li et al. (2018)
31	SPR	Molecularly imprinted polypyrolle	0.3–3000 ng/mL	0.3 ng/g	Choi et al. (2009)
32	SPR	Competitive inhibition enzyme-linked immunoassay (CI-ELISA)	0.002–2.5 μg/mL	8 ng/mL	Edupuganti et al. (2013)
33	iSPR	Competitive inhibition, immunoassay	0.01–1000 ng/mL	6 ng/mL	Joshi et al. (2016)
34	iSPR	AuNP enhanced iSPR competitive immunoassay	102–835 ng/g	57 ng/g	Hossain and Maragos (2018)
35	iSPR	Competitive inhibition, immunoassay	~1–1000 ng/mL (NR/from calibration graph)	10 ng/mL	Dorokhin et al. (2011)
36	AIR spectroscopic ellipsometry	Aptamer, and measurement under SPR conditions	0.01 ng/mL - 1000 ng/mL	0.08 ng/mL	this study

detection ranges were quite suitable (such as 0.01–10000 ng/mL) for food safety applications. As expected, electrochemical methods are quite sensitive and can operate a wider range of detection. Unfortunately, their selectivity and sensitivity should be fine-tuned using various tools such as magnetic beads, nanoparticles, nanotubes even core-shell particles to achieve better analytical performance (Hervàs et al., 2011; Riberi et al., 2018). Fluorescence methods, however, have higher LOD and quite narrower detection ranges. For example, an immunosensor assay based on microfluidics have quite lower LOD (0.01 ng/mL) while its calibration range is between 0.08 and 7.47 ng/mL (Wang et al., 2013). Colorimetric based sensors have also higher LOD and a narrower range of detection (for example (Liu et al., 2012)). Among these methods, SPR based methods have also quite higher LOD and narrower detection ranges. A quite number of these optical-based methods reported herein, also are immuno-assays.

Our AIR-SE method under SPR condition, was suitable for ZEN detection in food samples directly, without using any tag or additional sandwich assay approaches. Also, its analytical performance is high enough (e.g. nearly competitive to electrochemical methods) for ZEN detection in real samples. However, the suitability of this proposed method for using at the point of monitoring site (e.g. at marketplaces) is not good enough due to the technical limitations in regard to the miniaturization of ellipsometry.

Author contribution ctatement

M.Oguzhan Caglayan: Data curation, Conceptualization, Writing, Methodology, Investigation, Software, Visualization, Supervision, Writing - Original Draft and Writing - Review & Editing.

Zafer Ustundag: Writing, Methodology, Data curation, Investigation, Validation, Formal analysis, Writing - Original Draft.

Declaration of competing interest

The authors declare that they have no known competing financial interests or personal relationships that could have appeared to influence the work reported in this paper.

Acknowledgment

This work was financially supported by the Kutahya Dumlupinar University Scientific Research Fund with a Grant number of 2011–27.

References

Afzali, D., Padash, M., Mostafavi, A., 2015. Determination of trace amounts of zearalenone in beverage samples with an electrochemical sensor. Mycotoxin Res. 31, 203–208.
Alshannaq, A., Yu, J.-H., 2017. Occurrence, toxicity, and analysis of major mycotoxins in food. Int. J. Environ. Res. Public Health 14, 632.
Bennett, J.W., Klich, M., 2003. Mycotoxins. Clin. Microbiol. Rev. 16, 497–516.
Bombarová, K., Chlpík, J., Cirák, J., 2015. Surface plasmon resonance ellipsometry based biosensor for the investigation of biomolecular interactions. Mater. Today: Proc. 2, 70–76.
Caglayan, M.O., 2018. Plasmon resonance-enhanced internal reflection ellipsometry for the trace detection of mercuric ion. Int. J. Environ. Sci. Technol. 15, 909–914.
Caglayan, M.O., Atar, N., Zafer, U., 2013. Surface plasmon resonance biosensors: sensor response modeling. J. Comput. Theor. Nanosci. 10, 1248–1251.
Chauhan, R., Singh, J., Sachdev, T., Basu, T., Malhotra, B.D., 2016. Recent advances in mycotoxins detection. Biosens. Bioelectron. 81, 532–545.
Chen, X., Huang, Y., Duan, N., Wu, S., Ma, X., Xia, Y., Zhu, C., Jiang, Y., Wang, Z., 2013. Selection and identification of ssDNA aptamers recognizing zearalenone. Anal. Bioanal. Chem. 405, 6573–6581.
Chen, X., Shen, C., Qu, B., 2017. Determination of 16 mycotoxins in vegetable oils using a QuEChERS method combined with high-performance liquid chromatography-tandem mass spectrometry AU - zhao, Hongxia. Food Addit. Contam. A 34, 255–264.
Choi, S.-W., Chang, H.-J., Lee, N., Kim, J.-H., Chun, H.S., 2009. Detection of mycoestrogen zearalenone by a molecularly imprinted polypyrrole-based surface plasmon resonance (SPR) sensor. J. Agric. Food Chem. 57, 1113–1118.
Chun, H.S., Choi, E.H., Chang, H.J., Choi, S.W., Eremin, S.A., 2009. A fluorescence polarization immunoassay for the detection of zearalenone in corn. Anal. Chim. Acta 639, 83–89.
Collins, T.F.X., Sprando, R.L., Black, T.N., Olejnik, N., Eppley, R.M., Alam, H.Z., Rorie, J., Ruggles, D.I., 2006. Effects of zearalenone on in utero development in rats. Food Chem. Toxicol. 44, 1455–1465.
Daly, S.J., Keating, G.J., Dillon, P.P., Manning, B.M., O'Kennedy, R., Lee, H.A., Morgan, M.R.A., 2000. Development of surface plasmon resonance-based immunoassay for aflatoxin B1. J. Agric. Food Chem. 48, 5097–5104.
Dorokhin, D., Haasnoot, W., Franssen, M.C.R., Zuilhof, H., Nielen, M.W.F., 2011. Imaging surface plasmon resonance for multiplex microassay sensing of mycotoxins. Anal. Bioanal. Chem. 400, 3005–3011.
Edupuganti, S.R., Edupuganti, O.P., O'Kennedy, R., 2013. Generation of anti-zearalenone scFv and its incorporation into surface plasmon resonance-based assay for the detection of zearalenone in sorghum. Food Control 34, 668–674.
Fernández, H., Arévalo, F.J., Granero, A.M., Robledo, S.N., Nieto, C.H.D., Riberi, W.I., Zon, M.A., 2017. Electrochemical biosensors for the determination of toxic substances related to food safety developed in South America: mycotoxins and herbicides. Chemosensors 5, 23.
Goud, K.Y., Kalisa, S.K., Kumar, V., Tsang, Y.F., Lee, S.E., Gobi, K.V., Kim, K.H., 2018. Progress on nanostructured electrochemical sensors and their recognition elements for detection of mycotoxins: a review. Biosens. Bioelectron. 121, 205–222.
Gu, W., Zhu, P., Jiang, D., He, X., Li, Y., Ji, J., Zhang, L., Sun, Y., Sun, X., 2015. A novel and simple cell-based electrochemical impedance biosensor for evaluating the combined toxicity of DON and ZEN. Biosens. Bioelectron. 70, 447–454.
Hervas, M., Lopez, M.A., Escarpa, A., 2009. Electrochemical immunoassay using magnetic beads for the determination of zearalenone in baby food: an anticipated analytical tool for food safety. Anal. Chim. Acta 653, 167–172.
Hervas, M., Lopez, M.A., Escarpa, A., 2010. Simplified calibration and analysis on screen-printed disposable platforms for electrochemical magnetic bead-based immunosensing of zearalenone in baby food samples. Biosens. Bioelectron. 25, 1755–1760.
Hervás, M., López, M.A., Escarpa, A., 2011. Integrated electrokinetic magnetic bead-based electrochemical immunoassay on microfluidic chips for reliable control of permitted levels of zearalenone in infant foods. Analyst 136, 2131–2138.
Hervás, M., López, M.Á., Escarpa, A., 2009. Electrochemical microfluidic chips coupled to magnetic bead-based ELISA to control allowable levels of zearalenone in baby foods using simplified calibration. Analyst 134, 2405–2411.
Hossain, M.Z., Maragos, C.M., 2018. Gold nanoparticle-enhanced multiplexed imaging surface plasmon resonance (iSPR) detection of Fusarium mycotoxins in wheat. Biosens. Bioelectron. 101, 245–252.
Ji, J., Gu, W., Sun, C., Sun, J., Jiang, H., Zhang, Y., Sun, X., 2016. A novel recombinant cell fluorescence biosensor based on toxicity of pathway for rapid and simple evaluation of DON and ZEN. Sci. Rep. 6.
Joshi, S., Segarra-Fas, A., Peters, J., Zuilhof, H., van Beek, T.A., Nielen, M.W.F., 2016. Multiplex surface plasmon resonance biosensing and its transferability towards imaging nanoplasmonics for detection of mycotoxins in barley. Analyst 141, 1307–1318.
Kabak, B., 2009. The fate of mycotoxins during thermal food processing. J. Sci. Food Agric. 89, 549–554.
Lee, B., Park, J.H., Byun, J.Y., Kim, J.H., Kim, M.G., 2018. An optical fiber-based LSPR aptasensor for simple and rapid in-situ detection of ochratoxin A. Biosens. Bioelectron. 102, 504–509.
Li, P., Zhang, Z., Zhang, Q., Zhang, N., Zhang, W., Ding, X., Li, R., 2012. Current development of microfluidic immunosensing approaches for mycotoxin detection via capillary electromigration and lateral flow technology. Electrophoresis 33, 2253–2265.
Li, X., Li, P., Zhang, Q., Li, R., Zhang, W., Zhang, Z., Ding, X., Tang, X., 2013. Multicomponent immunochromatographic assay for simultaneous detection of aflatoxin B1, ochratoxin A and zearalenone in agro-food. Biosens. Bioelectron. 49, 426–432.
Li, Y., Chen, Q., Xu, X., Jin, Y., Wang, Y., Zhang, L., Yang, W., He, L., Feng, X., Chen, Y., 2018. Microarray surface enhanced Raman scattering based immunosensor for multiplexing detection of mycotoxin in foodstuff. Sens. Actuators B Chem. 266, 115–123.
Liu, B., Wang, F., Ma, X., Li, Z., Guo, D., Wang, Y., Wan, F., Deng, L., Zhang, S., 2018. Determination of 16 mycotoxins in maize by ultrahigh-performance liquid chromatography–tandem mass spectrometry AU - Li, Xia. Anal. Lett. 51, 702–716.
Liu, G., Han, Z., Nie, D., Yang, J., Zhao, Z., Zhang, J., Li, H., Liao, Y., Song, S., De Saeger, S., Wu, A., 2012. Rapid and sensitive quantitation of zearalenone in food and feed by lateral flow immunoassay. Food Control 27, 200–205.
Liu, L., Chao, Y., Cao, W., Wang, Y., Luo, C., Pang, X., Fan, D., Wei, Q., 2014. A label-free amperometric immunosensor for detection of zearalenone based on trimetallic Au-core/AgPt-shell nanorattles and mesoporous carbon. Anal. Chim. Acta 847, 29–36.
Liu, N., Chen, S., Li, Y., Dai, H., Lin, Y., 2017. Self-enhanced photocathodic matrix based on poly-dopamine sensitized TiO2 mesocrystals for mycotoxin detection assisted by a dual amplificatory nanotag. New J. Chem. 41, 3380–3386.
Llorent-Martínez, E.J., Fernández-Poyatos, M.P., Ruiz-Medina, A., 2019. Automated fluorimetric sensor for the determination of zearalenone mycotoxin in maize and cereals feedstuff. Talanta 191, 89–93.
Mak, A.C., Osterfeld, S.J., Yu, H., Wang, S.X., Davis, R.W., Jejelowo, O.A., Pourmand, N., 2010. Sensitive giant magnetoresistive-based immunoassay for multiplex mycotoxin detection. Biosens. Bioelectron. 25, 1635–1639.
Man, Y., Liang, G., Li, A., Pan, L., 2017. Recent advances in mycotoxin determination for food monitoring via microchip. Toxins 9, 324.
Maragos, C.M., Appell, M., 2007. Capillary electrophoresis of the mycotoxin zearalenone using cyclodextrin-enhanced fluorescence. J. Chromatogr. A 1143, 252–257.
Meneely, J.P., Elliott, C.T., 2014. Rapid surface plasmon resonance immunoassays for the determination of mycotoxins in cereals and cereal-based food products. World Mycotoxin J. 7, 491–505.
Nasir, M.Z.M., Pumera, M., 2014. Mycotoxins: simultaneous detection of zearalenone and

citrinin by voltammetry on edge plane pyrolytic graphite electrode. Electroanalysis 26, 1901–1904.
Orlov, A.V., Burenin, A.G., Massarskaya, N.G., Betin, A.V., Nikitin, M.P., Nikitin, P.I., 2017. Highly reproducible and sensitive detection of mycotoxins by label-free biosensors. Sens. Actuators B Chem. 246, 1080–1084.
Panini, N.V., Salinas, E., Messina, G.A., Raba, J., 2011. Modified paramagnetic beads in a microfluidic system for the determination of zearalenone in feedstuffs samples. Food Chem. 125, 791–796.
Peters, J., Thomas, D., Boers, E., de Rijk, T., Berthiller, F., Haasnoot, W., Nielen, M.W.F., 2013. Colour-encoded paramagnetic microbead-based direct inhibition triplex flow cytometric immunoassay for ochratoxin A, fumonisins and zearalenone in cereals and cereal-based feed. Anal. Bioanal. Chem. 405, 7783–7794.
Ren, G., Hu, Y., Zhang, J., Zou, L., Zhao, G., 2018. Determination of multi-class mycotoxins in tartary buckwheat by ultra-fast liquid chromatography coupled with triple quadrupole mass spectrometry. Toxins 10, 28.
Riberi, W.I., Tarditto, L.V., Zon, M.A., Arévalo, F.J., Fernández, H., 2018. Development of an electrochemical immunosensor to determine zearalenone in maize using carbon screen printed electrodes modified with multi-walled carbon nanotubes/polyethyleneimine dispersions. Sens. Actuators B Chem. 254, 1271–1277.
Rodrigues, I., Handl, J., Binder, E.M., 2011. Mycotoxin occurrence in commodities, feeds and feed ingredients sourced in the Middle East and Africa. Food Addit. Contam. Part B, Surveillance 4, 168–179.
Sharma, R., Ragavan, K.V., Thakur, M.S., Raghavarao, K.S.M.S., 2015. Recent advances in nanoparticle based aptasensors for food contaminants. Biosens. Bioelectron. 74, 612–627.
Shephard, G.S., 2008. Determination of mycotoxins in human foods. Chem. Soc. Rev. 37, 2468–2477.
Sun, S., Zhao, R., Feng, S., Xie, Y., 2018. Colorimetric zearalenone assay based on the use of an aptamer and of gold nanoparticles with peroxidase-like activity. Microchim. Acta 185, 535.
Tuerk, C., 1997. Using the SELEX combinatorial chemistry process to find high affinity nucleic acid ligands to target molecules. Methods Mol. Biol. 67, 219–230.
Urraca, J.L., Benito-Peña, E., Pérez-Conde, C., Moreno-Bondi, M.C., Pestka, J.J., 2005. Analysis of zearalenone in cereal and swine feed samples using an automated flow-through immunosensor. J. Agric. Food Chem. 53, 3338–3344.
Vlata, Z., Porichis, F., Tzanakakis, G., Tsatsakis, A., Krambovitis, E., 2006. A study of zearalenone cytotoxicity on human peripheral blood mononuclear cells. Toxicol. Lett. 165, 274–281.
Wang, Y.-K., Yan, Y.-X., Mao, Z.-W., Wang, H.-a., Zou, Q., Hao, Q.-W., Ji, W.-H., Sun, J.-H., 2013. Highly sensitive electrochemical immunoassay for zearalenone in grain and grain-based food. Microchim. Acta 180, 187–193.
Wang, Y., Liu, N., Ning, B., Liu, M., Lv, Z., Sun, Z., Peng, Y., Chen, C., Li, J., Gao, Z., 2012. Simultaneous and rapid detection of six different mycotoxins using an immunochip. Biosens. Bioelectron. 34, 44–50.
Wu, W., Zhu, Z., Li, B., Liu, Z., Jia, L., Zuo, L., Chen, L., Zhu, Z., Shan, G., Luo, S.Z., 2018. A direct determination of AFBs in vinegar by aptamer-based surface plasmon resonance biosensor. Toxicon 146, 24–30.
Wu, Z., Xu, E., Chughtai, M.F.J., Jin, Z., Irudayaraj, J., 2017. Highly sensitive fluorescence sensing of zearalenone using a novel aptasensor based on upconverting nanoparticles. Food Chem. 230, 673–680.
Xia, S., Zhu, P., Pi, F., Zhang, Y., Li, Y., Wang, J., Sun, X., 2017. Development of a simple and convenient cell-based electrochemical biosensor for evaluating the individual and combined toxicity of DON, ZEN, and AFB1. Biosens. Bioelectron. 97, 345–351.
Xu, W., Qing, Y., Chen, S., Chen, J., Qin, Z., Qiu, J., Li, C., 2017. Electrochemical indirect competitive immunoassay for ultrasensitive detection of zearalenone based on a glassy carbon electrode modified with carboxylated multi-walled carbon nanotubes and chitosan. Microchim. Acta 184, 3339–3347.
Yan, Z., Wang, L., Wang, J., Tan, Y., Yu, D., Chang, X., Fan, Y., Zhao, D., Wang, C., De Boevre, M., De Saeger, S., Sun, C., Wu, A., 2018. A QuEChERS-based liquid chromatography-tandem mass spectrometry method for the simultaneous determination of nine zearalenone-like mycotoxins in pigs. Toxins 10, 129.
Yang, C., Wang, Y., Marty, J.L., Yang, X., 2011. Aptamer-based colorimetric biosensing of Ochratoxin A using unmodified gold nanoparticles indicator. Biosens. Bioelectron. 26, 2724–2727.
Zhang, X., Wang, X., Sun, M., Zhang, X., Song, H., Yan, Y., Sun, J., Li, X., Fang, W., 2015. A magnetic nanoparticle based enzyme-linked immunosorbent assay for sensitive quantification of zearalenone in cereal and feed samples. Toxins 7, 4216.
Zinedine, A., Soriano, J.M., Molto, J.C., Manes, J., 2007. Review on the toxicity, occurrence, metabolism, detoxification, regulations and intake of zearalenone: an oestrogenic mycotoxin. Food Chem. Toxicol. : Int. J. Publ. Br. Ind. Biol. Res. Assoc. 45, 1–18.
Zhan, S., Huang, X., Chen, R., Li, J., Xiong, Y., 2016. Novel fluorescent ELISA for the sensitive detection of zearalenone based on H 2 O 2-sensitive quantum dots for signal transduction. Talanta 158, 51–56.